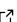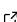# QhX: A Python package for periodicity detection in red noise

Andjelka B. Kovačević [1]*¶**, Dragana Ilić** [1]**, Momčilo Tošić**[1]***, Marina Pavlović** [2]**, Aman Raju** [1]**, Mladen Nikolić** [1]**, Saša Simić** [3]**, Iva Čvorović Hajdinjak** [1]**, and Luka Č. Popović** [4]

1 University of Belgrade-Faculty of Mathematics, Studentski trg 16, Belgrade, Serbia **2** Mathematical Institute of Serbian Academy of Science and Arts, Serbia **3** Faculty of sciences, University of Kragujevac, Radoja Domanovića 12, Serbia **4** Astronomical Observatory, Belgrade, Serbia ¶ Corresponding author * These authors contributed equally.

Summary

QhX is a Python package for detecting periodicity in red noise time series, developed as an in-kind contribution to the Vera C. Rubin Observatory Legacy Survey of Space and Time (LSST, Ivezić et al., 2019). Traditional Fourier-based methods often struggle with red noise, which is common in quasar light curves and other accreting objects. QhX addresses these challenges with its core 2D Hybrid method (Kovačević et al., 2018). Input data are mapped into a time-period plane via wavelet transforms, which are (auto)correlated to produce a correlation density map in a "period-period" plane. Statistical vetting incorporates significance, upper and lower error bounds, and the novel Intersection over Union (IoU) metric to evaluate the proximity and overlap of detected periods across bands and objects. In addition to a vetted numerical catalog, QhX dynamically visualizes periodicity across photometric bands and objects.

Statement of need
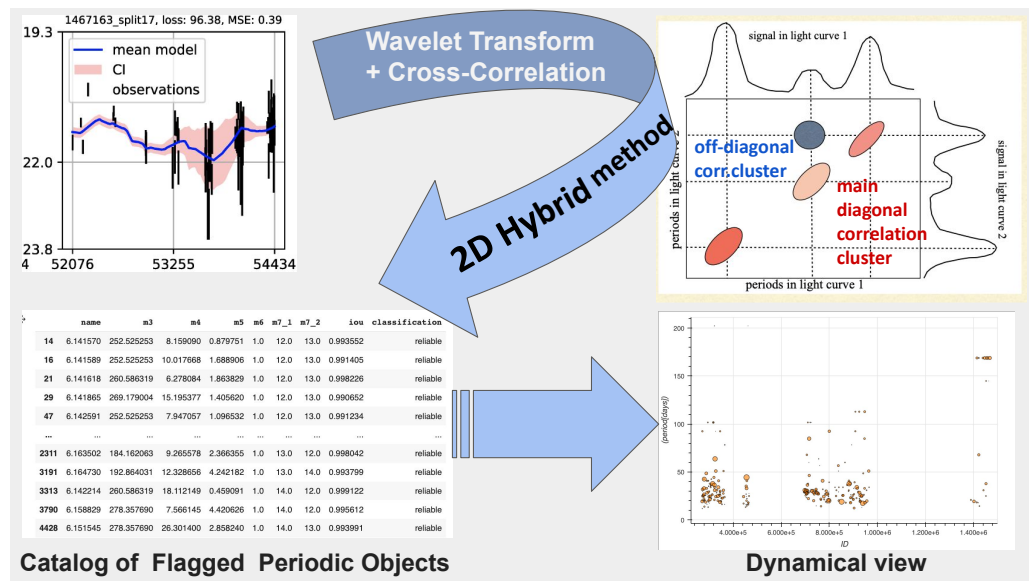
Figure 1: The left panel shows a 1D light curve with observational data (black error bars) and a model (blue line). QhX transforms the time-series into the time-frequency domain and cross-correlates wavelet matrices to produce a 2D period-period correlation map (right), where clusters indicate periodic signals. After map integration, statistical vetting generates a numerical catalog of flagged periodic objects (bottom left) and a dynamic view of detected periods across objects and bands (bottom right).

Periodic variability spans a range of astronomical objects, from asteroids to quasars. Identifying meaningful signals is complicated by red noise (see, e.g., Figure 1 in Gaia Collaboration et al., 2019; Kasliwal et al., 2015; Kovačević, Radović, et al., 2022), which exhibits fractal-like patterns across time scales (Belete et al., 2018; Vio et al., 1991). Non-stationary signals and unfavorable sampling (Brandt et al., 2018; D'Orazio & Charisi, 2023) further obscure coherent patterns. Traditional time-frequency methods, constrained by the Fourier uncertainty principle (i.e., Gabor limit, Gabor, 1947), often fail with such complex signals, highlighting the need for nonlinear approaches (Abry et al., 1995; Cohen, 1995).

QhX provides features specifically designed to address these challenges. The first feature is its core 2D Hybrid method (see Figure 1), detailed in (Kovačević et al., 2018), inspired by 2D Correlation Spectroscopy (Kovačević, 2024; Noda, 2018). By applying wavelet transforms, QhX maps time-series data into the time-frequency domain and (auto)correlates it, generating a period-period correlation density that enhances signal detection. Secondly, QhX introduces an Intersection over Union (IoU) metric, combined with standard statistical measures (significance, upper and lower error bounds), to evaluate the overlap of detected periods across bands and objects. Each period is represented as the center of an "IoU ball," with its radius reflecting relative error, calculated as the mean of the upper and lower error bounds—analogous to a circular aperture in photometry (Saxena et al., 2024). Thirdly, QhX enhances traditional analysis by generating numerical and interactive visual catalogs that rank periodicity candidates by reliability. These interactive catalogs enable detailed inspection of signal consistency, offering greater interpretability than traditional static plots.
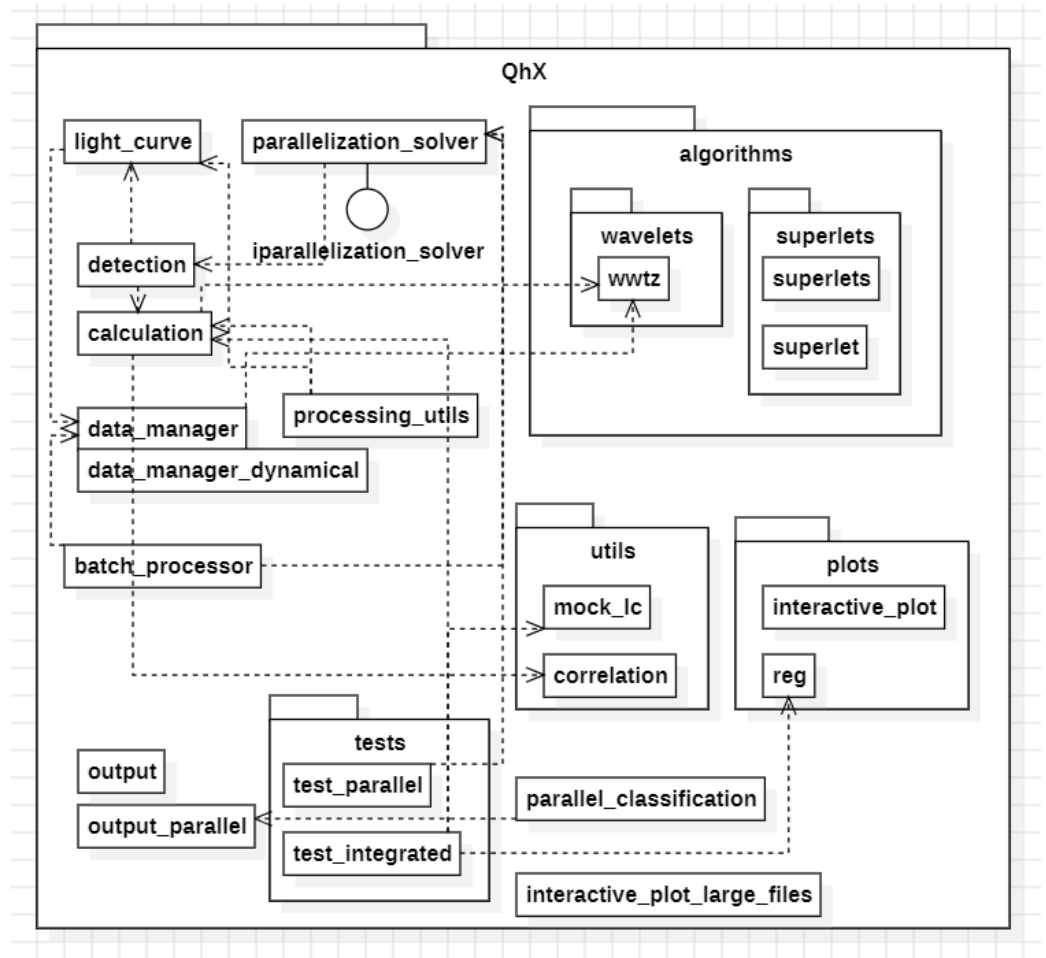
QhX structure

Figure 2: Schematic representation of the QhX package architecture.

QhX (Version 0.2.0) is an open-source package optimized for gappy quasar light curves but adaptable to other datasets. It supports both dynamic and fixed modes, with parallel processing capabilities for large-scale data. The modular design facilitates rapid experimentation by enabling easy swapping or modification of functions (see Figure 2), addressing diverse research needs. For fixed-only workflows, specialized functions such as data_manager offer minimal overhead and optimal performance, while data_manager_dynamical supports both dynamic and fixed configurations to handle more complex scenarios involving dynamic filters.

The package is organized as follows:

1. **Core**:
   - algorithms module provides essential signal-processing techniques, including the Weighted Wavelet Z-Transform (wwtz) and prototype superlet transforms.
   - correlation function within the utils module supports the 2D Hybrid method by converting light curve data into wavelet matrices and performing (auto)correlation, creating correlation density.
2. **Signal Detection and Validation**:
   - detection module identifies candidate periodic signals and assesses their validity using statistical measures (significance and upper and lower error (Johnson et al., 2019)). The Intersection over Union (IoU) metric identifies overlapping periods

across bands and objects. To our knowledge, this is the first application of the Intersection-over-Union (IoU) metric to quantify the overlap between detected and reference periods in astronomical time-series analysis.

- Statistical vetting categorizes detected periods for each object and band as reliable, medium, or poor.

3. **Data Management**:
   - QhX assumes input time-series data in a simple tabular format containing time, flux (or magnitude), and associated uncertainties. Examples in the documentation illustrate how to map data from other commonly used formats into this structure.
   - `data_manager` and `data_manager_dynamical` modules manage data flow, data loading, outlier removal, and format compatibility.
   - `batch_processor` and `parallelization_solver` modules optimize task distribution across multiple processors.

4. **Visualization and Output**:
   - `plots` module includes tools for creating interactive visualizations, such as `interactive_plot`, which allows for exploring detected periodicities across bands and objects. For large datasets, `interactive_plot_large_files` enables in-depth inspection of signal consistency.
   - `output` and `output_parallel` modules handle result storage, supporting both single-threaded and parallelized workflows.

5. **Testing**:
   - `tests` module, containing `test_parallel` and `test_integrated`, validates the functionality across various processing setups.

Representative Applications

QhX has been benchmarked with respect to widely used periodicity detection software across multiple domains. In Fatović et al. (2023), applying QhX to SDSS J2320$+$0024 yielded a period of $278.36^{+57.34}_{-25.21}$ days, with a significance above 99% measured via the shuffling method, and a 90% significance from the Generalized Extreme Value (GEV) approach. A Lomb–Scargle periodogram applied to the same dataset produced a consistent period of 278~days at the same significance level. In Kovačević et al. (2019), QhX detected periods of 1972 ± 254~days (observed light curve) and 1873 ± 250 days (modeled light curve) for PG~1302–102, both within 1σ of the 1884 ± 88 day period reported by Graham et al. (2015) using generalized Lomb–Scargle, wavelet, and autocorrelation methods; a Bayesian reanalysis by Zhu & Thrane (2020) on an extended dataset for PG~1302–102 yielded a comparable quasi-period of 5.6 yr, interpreted as quasiperiodic oscillations. In the case of Mrk 231 (Kovačević, Yi, et al., 2020), the 2D hybrid method identified a characteristic period of 403 days with a significance greater than 99.7%, in agreement with a Lomb–Scargle periodogram result of 413 days at a significance above 95%; the slightly larger uncertainty in the QhX-derived period reflects the temporal variation of the periodicity, while the average oscillation power is comparable between the two methods. The method has also been validated in the context of damped oscillations in the changing-look quasar NGC 3516 (Kovačević, Popović, et al., 2020), where experimental results demonstrated robustness against the combined effects of red noise and complex time-series structure. Beyond astrophysical applications, QhX has been applied to Very Low Frequency (VLF) signal analysis for pre- and post-earthquake intervals (Kovačević, Nina, et al., 2022). In the no-earthquake scenario (same date one year earlier), the topology of QhX 2D hybrid maps exhibited distinct correlation cluster patterns compared to earthquake-day records, with detected periods below 111 s in most intervals and a ~ 140 s signal in the -2 h segment, closely matching a 147 s signal detected during the earthquake event. Comparison with Fast Fourier Transform (FFT) results (Nina et al., 2020) showed strong agreement before the earthquake for periods below 1.5 min, and convergence of both methods to similar values in subsequent intervals. Post-earthquake periods obtained with QhX were also consistent with the < 10s to few-hundred-second range reported in (Ohya et al., 2018). QhX is the LSST

114 directable software in-kind contribution.

Acknowledgements

References

Abry, P., Gonçalvès, P., & Flandrin, P. (1995). *Wavelets, spectrum analysis and 1/f processes* (A. Antoniadis & G. Oppenheim, Eds.; pp. 15–29). Springer New York. https://doi.org/10.1007/978-1-4612-2544-7_2

Belete, A. B., Bravo, J. P., Canto Martins, B. L., Leão, I. C., De Araujo, J. M., & De Medeiros, J. R. (2018). Multifractality signatures in quasars time series - I. 3C 273. *478*(3), 3976–3986. https://doi.org/10.1093/mnras/sty1316

Brandt, W. N., Ni, Q., Yang, G., Anderson, S. F., Assef, R. J., Barth, A. J., Bauer, F. E., Bongiorno, A., Chen, C.-T., De Cicco, D., Gezari, S., Grier, C. J., Hall, P. B., Hoenig, S. F., Lacy, M., Li, J., Luo, B., Paolillo, M., Peterson, B. M., … Yu, Z. (2018). Active Galaxy Science in the LSST Deep-Drilling Fields: Footprints, Cadence Requirements, and Total-Depth Requirements. *arXiv e-Prints*, arXiv:1811.06542. https://doi.org/10.48550/arXiv.1811.06542

Cohen, L. (1995). *Time-frequency analysis*. Prentice Hall PTR. ISBN: 9780135945322

D'Orazio, D. J., & Charisi, M. (2023). Observational Signatures of Supermassive Black Hole Binaries. *arXiv e-Prints*, arXiv:2310.16896. https://doi.org/10.48550/arXiv.2310.16896

Fatović, M., Palaversa, L., Tisanić, K., Thanjavur, K., Ivezić, Ž., Kovačević, A. B., Ilić, D., & Č. Popović, L. (2023). Detecting Long-period Variability in the SDSS Stripe 82 Standards Catalog. *165*(4), 138. https://doi.org/10.3847/1538-3881/acb596

Gabor, D. (1947). Acoustical quanta and the theory of hearing. *Nature*, *159*(4044), 591–594. https://doi.org/10.1038/159591a0

Gaia Collaboration, Eyer, L., Rimoldini, L., Audard, M., Anderson, R. I., Nienartowicz, K., Glass, F., Marchal, O., Grenon, M., Mowlavi, N., Holl, B., Clementini, G., Aerts, C., Mazeh, T., Evans, D. W., Szabados, L., Brown, A. G. A., Vallenari, A., Prusti, T., … Zwitter, T. (2019). Gaia Data Release 2. Variable stars in the colour-absolute magnitude diagram. *Astronomy & Astrophysics*, *623*, A110. https://doi.org/10.1051/0004-6361/201833304

Graham, M. J., Djorgovski, S. G., Stern, D., Glikman, E., Drake, A. J., Mahabal, A. A., Donalek, C., Larson, S., & Christensen, E. (2015). A possible close supermassive black-hole binary in a quasar with optical periodicity. *518*(7537), 74–76. https://doi.org/10.1038/nature14143

Ivezić, Ž., Kahn, S. M., Tyson, J. A., Abel, B., Acosta, E., Allsman, R., Alonso, D., AlSayyad, Y., Anderson, S. F., Andrew, J., Angel, J. R. P., Angeli, G. Z., Ansari, R., Antilogus, P., Araujo, C., Armstrong, R., Arndt, K. T., Astier, P., Aubourg, É., … Zhan, H. (2019). LSST: From Science Drivers to Reference Design and Anticipated Data Products. *873*(2), 111. https://doi.org/10.3847/1538-4357/ab042c

Johnson, M. A. C., Gandhi, P., Chapman, A. P., Moreau, L., Charles, P. A., Clarkson, W. I., & Hill, A. B. (2019). Prospecting for periods with LSST - low-mass X-ray binaries as a test case. *Monthly Notices of the Royal Astronomical Society*, *484*(1), 19–30.

158   https://doi.org/10.1093/mnras/sty3466

159 Kasliwal, V. P., Vogeley, M. S., & Richards, G. T. (2015). Are the variability properties of the
160   Kepler AGN light curves consistent with a damped random walk? *Monthly Notices of the*
161   *Royal Astronomical Society*, *451*(4), 4328–4345. https://doi.org/10.1093/mnras/stv1230

162 Kovačević, A. B. (2024). Two-dimensional (2D) hybrid method: Expanding 2D corre-
163   lation spectroscopy (2D-COS) for time series analysis. *Applied Spectroscopy*, *0*(0),
164   00037028241241308. https://doi.org/10.1177/00037028241241308

165 Kovačević, A. B., Nina, A., Popović, L. Č., & Radovanović, M. (2022). Two-dimensional
166   correlation analysis of periodicity in noisy series: Case of VLF signal amplitude variations
167   in the time vicinity of an earthquake. *Mathematics*, *10*(22). https://doi.org/10.3390/
168   math10224278

169 Kovačević, A. B., Pérez-Hernández, E., Popović, L. Č., Shapovalova, A. I., Kollatschny, W., &
170   Ilić, D. (2018). Oscillatory patterns in the light curves of five long-term monitored type 1
171   active galactic nuclei. *475*(2), 2051–2066. https://doi.org/10.1093/mnras/stx3137

172 Kovačević, A. B., Popović, L. Č., & Ilić, D. (2020). Two-dimensional correlation analysis of
173   periodicity in active galactic nuclei time series. *Open Astronomy*, *29*(1), 51–55. https:
174   //doi.org/10.1515/astro-2020-0007

175 Kovačević, A. B., Popović, L. Č., Simić, S., & Ilić, D. (2019). The Optical Variability of
176   Supermassive Black Hole Binary Candidate PG 1302-102: Periodicity and Perturbation in
177   the Light Curve. *871*(1), 32. https://doi.org/10.3847/1538-4357/aaf731

178 Kovačević, A. B., Radović, V., Ilić, D., Popović, L. Č., Assef, R. J., Sánchez-Sáez, P., Nikutta,
179   R., Raiteri, C. M., Yoon, I., Homayouni, Y., Li, Y.-R., Caplar, N., Czerny, B., Panda, S.,
180   Ricci, C., Jankov, I., Landt, H., Wolf, C., Kovačević-Dojčinović, J., … Marčeta-Mandić, S.
181   (2022). The LSST Era of Supermassive Black Hole Accretion Disk Reverberation Mapping.
182   *262*(2), 49. https://doi.org/10.3847/1538-4365/ac88ce

183 Kovačević, A. B., Yi, T., Dai, X., Yang, X., Čvorović-Hajdinjak, I., & Popović, L. Č. (2020).
184   Confirmed short periodic variability of subparsec supermassive binary black hole candidate
185   Mrk 231. *494*(3), 4069–4076. https://doi.org/10.1093/mnras/staa737

186 Nina, A., Pulinets, S., Biagi, P. F., Nico, G., Mitrović, S. T., Radovanović, M., & Popović, L.
187   Č. (2020). Variation in natural short-period ionospheric noise, and acoustic and gravity
188   waves revealed by the amplitude analysis of a VLF radio signal on the occasion of the
189   kraljevo earthquake (mw= 5.4). *Science of the Total Environment*, *710*, 136406.

190 Noda, I. (2018). Chapter 2 - advances in two-dimensional correlation spectroscopy (2DCOS).
191   In J. Laane (Ed.), *Frontiers and advances in molecular spectroscopy* (pp. 47–75). Elsevier.
192   https://doi.org/https://doi.org/10.1016/B978-0-12-811220-5.00002-2

193 Ohya, H., Tsuchiya, F., Takishita, Y., Shinagawa, H., Nozaki, K., & Shiokawa, K. (2018).
194   Periodic oscillations in the d region ionosphere after the 2011 tohoku earthquake using LF
195   standard radio waves. *Journal of Geophysical Research: Space Physics*, *123*(6), 5261–5270.

196 Saxena, A., Salvato, M., Roster, W., Shirley, R., Buchner, J., Wolf, J., Kohl, C., Starck, H.,
197   Dwelly, T., Comparat, J., & al., et. (2024). CIRCLEZ : Reliable photometric redshifts for
198   active galactic nuclei computed solely using photometry from Legacy Survey Imaging for
199   DESI. *690*, A365. https://doi.org/10.1051/0004-6361/202450886

200 Vio, R., Cristiani, S., Lessi, O., & Salvadori, L. (1991). 3C 345: Is the Variability of Quasars
201   Nonlinear? *380*, 351. https://doi.org/10.1086/170594

202 Zhu, X.-J., & Thrane, E. (2020). Toward the Unambiguous Identification of Supermassive
203   Binary Black Holes through Bayesian Inference. *900*(2), 117. https://doi.org/10.3847/
204   1538-4357/abac5a